Laser-assisted in-flight muon-catalyzed deuteron-triton fusion

Shiwei Liu [1], Difa Ye [2], and Jie Liu [3,4,*]

[1] *Beijing Computational Science Research Center, Beijing 100193, People's Republic of China*
[2] *Laboratory of Computational Physics, Institute of Applied Physics and Computational Mathematics, Beijing 100088, People's Republic of China*
[3] *Graduate School, China Academy of Engineering Physics, Beijing 100193, People's Republic of China*
[4] *HEDPS, Center for Applied Physics and Technology, and College of Engineering, Peking University, Beijing 100871, People's Republic of China*

(Received 9 September 2022; revised 15 November 2022; accepted 9 December 2022; published 23 December 2022)

We investigate the deuteron-triton (DT) fusion in a three-body collision system of Tμ (i.e, a muon bound to a triton) impacted by a deuteron in the presence of intense laser fields with a semiclassical (SC) method. In this model, the initial positions and momenta of triton and muon are sampled from microcanonical distribution, and the dynamical process of a deuteron with a given incident kinetic energy colliding with the Tμ atom is simulated by tracing the classical trajectories in the combined Coulomb potentials and laser fields. At the minimum distance between the deuteron and triton, quantum tunneling through the Coulomb barrier emerges, and the penetrability can be estimated with the Wentzel-Kramers-Brillouin formula. DT nuclear fusion occurs after this quantum tunneling, and the total fusion cross section takes the Gamow form. Within the framework of the SC model, we investigate the charge shielding effect, demonstrating that this effect emerges in the low energy regime, where the impact velocity of the deuteron is smaller than the average velocity of muons in the bound state. Furthermore, the tunneling penetrability is considerably enhanced because the deuteron closely approaches the triton due to the quiver motions of charged nuclei driven by intense laser fields. As a result, the fusion cross section in this in-flight muon catalyzed fusion system can be enhanced by up to six orders of magnitude. Moreover, we calculated the DT fusion sections for a wide range of laser parameters and obtained phase diagrams demonstrating the enhanced DT fusion. Finally, important implications in achieving a large number of fusion reactions catalyzed by muons assisted by laser fields are discussed.

DOI: 10.1103/PhysRevC.106.064611

I. INTRODUCTION

The deuteron-triton (DT) fusion reaction is a potential candidate for addressing sustainable and clean energy issues [1] that has attracted considerable attention in the study of controlled nuclear fusions, including magnetic confinement fusion [2–4] and inertial confinement fusion [5–7]. An important subject in fusion research is developing feasible approaches for enhancing DT fusion cross sections. Muon-catalyzed fusion (MCF) [8–11] and ultraintense laser field assisted fusion [12–16] are of interest schemes to consider.

The fusion reaction cross section can be parametrized by the widely accepted Gamow form [17]. The Gamow formula is proportional to the product of three factors, the geometrical cross section, the barrier transparency, and an astrophysical factor. The geometrical cross section depends on the de Broglie wavelength of the system. The barrier transparency indicates the penetration rate of a particle through a Coulomb barrier due to quantum tunneling effects [18–20]. The astrophysical factor describes the nuclear physics within the nuclear potential effective range [21].

In the traditional concept of MCF [22,23], DT fusion reactions can occur in pseudomolecules or pseudomolecular ions formed by muons immersed in mixtures of liquid deuterium and tritium. Since the muon mass is approximately 207 times larger than the electron mass, the barrier transparency and DT cross section in a muonic molecule may be increased by smaller equilibrium distances in electronic molecule [24–28]. However, experimental tests based on this concept are not achieved the balance between energy input required of muon production compared to the energy output of DT fusion due to the inadequate muon-catalyzed fusion cycles during its lifetime ($\tau_\mu \sim 2.2$ μs) [29–33]. Alternatively, some previous works have focused on muonic atom-nucleus collision cross sections, known as in-flight muon-catalyzed fusion (IFMCF), which appears to increase the muon-catalyzed fusion cycles to the necessary level [34–36].

Moreover, ultraintense laser fields have been shown to enhance DT fusion cross sections, providing a potential tool for manipulating the nuclear processes. Recent theoretical works [12,13] using the Floquet scattering theory method and the Kramers-Henneberger approximation approach have predicted that high-frequency lasers can increase the tunneling probability of DT fusion cross sections due to the Coulomb barrier suppression effect. The quantum Volkov

*jliu@gscaep.ac.cn

state approximation described in Ref. [14] shows that low-frequency lasers are effective for transferring field energy to DT systems and can therefore be applied to enhance fusion probabilities. More recently, a semiclassical (SC) method [16] was developed to investigate laser-assisted DT fusion. Compared to previous quantum methods, the SC approach has advantages in terms of readily implemented simulations and provides an intuitive picture of collision processes; thus, this approach can be applied to investigate DT fusion for a wide range of laser parameters in both the low-frequency and high-frequency regime.

In this paper, we extend the SC approach to investigate laser-assisted DT fusion in a muonic atom-nucleus collision system. We use the full-dimensional classical trajectory Monte Carlo (CTMC) approach to simulate the dynamics of the three-body collision between a muonic atom Tμ (a muon bound to a triton) impacted by a deuteron [37]. The minimum distance between DT nuclei can be determined by tracing the classical trajectories. At the nearest distance between the DT nuclei, the quantum tunneling penetrability can be calculated according to the Wentzel-Kramers-Brillouin (WKB) approximation [38]. Then, the DT fusion cross sections can be obtained by using the Gamow formula. Thus, we can apply the SC method to investigate the mechanism underlying the shielding effects of enhancing DT fusion cross sections at small incident energies of $\epsilon < 19.5$ keV. We find that the DT fusion probability in the IFMCF system can be increased for a certain range of laser parameters, especially for frequencies in the near-infrared regime, which are used in most intense laser facilities.

The remainder of this paper is organized as follows. Sec. II presents our SC model. In Sec. III, we discuss the mechanism of the IFMCF system and calculate the fusion cross sections of laser-assisted IFMCF. Finally, we present our conclusions in Sec. IV.

II. MODEL

We consider the scattering problem of the D-Tμ system [see Fig. 1(a)] with the CTMC approach [37]. The Hamiltonian of the three-body system can be written as

$$H = \frac{\boldsymbol{p}_{\rm D}^2}{2m_{\rm D}} + \frac{\boldsymbol{p}_{\rm T}^2}{2m_{\rm T}} + \frac{q_{\rm D}q_{\rm T}e^2}{4\pi\varepsilon_0|\boldsymbol{r}_{\rm D}-\boldsymbol{r}_{\rm T}|} + \frac{\boldsymbol{p}_{\mu}^2}{2m_{\mu}} - \frac{q_{\mu}q_{\rm T}e^2}{4\pi\varepsilon_0|\boldsymbol{r}_{\mu}-\boldsymbol{r}_{\rm T}|} - \frac{q_{\mu}q_{\rm D}e^2}{4\pi\varepsilon_0|\boldsymbol{r}_{\mu}-\boldsymbol{r}_{\rm D}|}, \quad (1)$$

where m_i and $q_i (i = \rm D, T, \text{and } \mu$ denote deuteron, triton, and muon, respectively) are the masses and charges of different particles, specified by $\boldsymbol{r}_i$ and $\boldsymbol{p}_i$, which are the position and momentum vectors, respectively. ε_0 is the vacuum dielectric constant. Since the muon mass is about 207 times larger than the electron mass, the Bohr radius and ground state energy of Tμ can be estimated as $a_\mu = \hbar^2/m_\rho e^2 \approx 265.66$ fm and $E_{\rm g.s.} = -m_\rho e^4/2\hbar^2 \approx -2.71$ keV according to simple scaling laws, where $m_\rho = m_\mu m_{\rm T}/(m_\mu + m_{\rm T})$ is the reduced mass of the muon and triton. The dynamics of the system are governed by the canonical equations $d\boldsymbol{r}_i/dt = \partial H/\partial \boldsymbol{p}_i$ and $d\boldsymbol{p}_i/dt = -\partial H/\partial \boldsymbol{r}_i$.

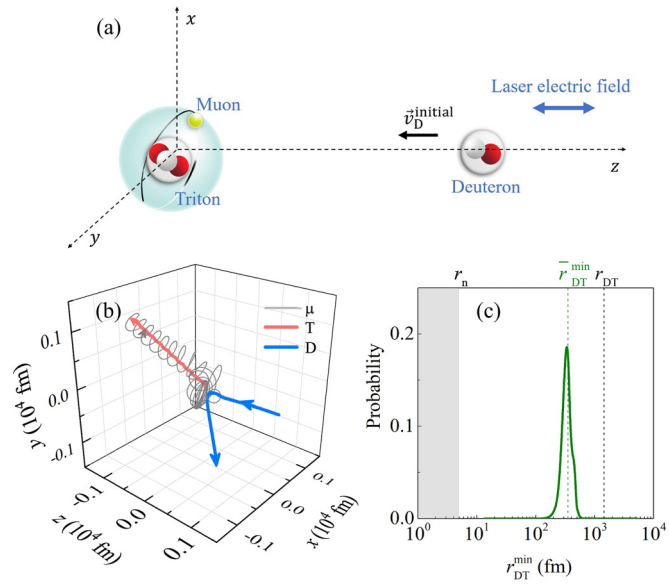

FIG. 1. (a) Schematic description of a muonic atom Tμ impacted by a deuteron in the presence of a strong laser field. (b) Typical classical trajectory of a D-Tμ collision. (c) The distribution of the minimum distance $r_{\rm DT}^{\rm min}$ between DT nuclei in a D-Tμ collision. The impact kinetic energy of deuteron is $\epsilon = 1$ keV. $r_{\rm DT} = 1441$ fm is the classical turning point of a bare DT collision with $\epsilon = 1$ keV, $r_{\rm n} = 3.89$ fm is the contact radius of the DT nuclei.

In our simulations, the initial positions and momenta of Tμ are sampled from the following microcanonical distribution:

$$\rho(\boldsymbol{r},\boldsymbol{p}) = \frac{\delta[E_{\rm g.s.} - H_{{\rm T}\mu}(\boldsymbol{r},\boldsymbol{p})]}{C}, \quad (2)$$

where $H_{{\rm T}\mu} = \boldsymbol{p}^2/2m_\rho - q_\mu q_{\rm T}e^2/4\pi\varepsilon_0|\boldsymbol{r}|$ represents the relative motion Hamiltonian of Tμ, $\boldsymbol{p} = |m_{\rm T}\boldsymbol{p}_\mu - m_\mu \boldsymbol{p}_{\rm T}|/(m_{\rm T} + m_\mu)$, and $\boldsymbol{r} = \boldsymbol{r}_\mu - \boldsymbol{r}_{\rm T}$. The constant C is introduced to normalize the distribution. Such microcanonical distribution is proposed by Abrines and Percival [39,40]. They use Kepler's equation of planetary motion to represent hydrogenic atoms with a randomly determined set of initial conditions, which constrained to yield the binding energy of the atom. The momentum distribution obtained by Eq. (2) totally agrees with the distribution calculated from quantum ground wave function as shown in Fig. 2,

$$\rho_{\boldsymbol{p}}(\boldsymbol{p}) = \frac{8p_c^2}{\pi^2\left(p^2 + p_c^2\right)^4}, \quad (3)$$

where $p_c = \sqrt{2m_\rho|E_{\rm g.s.}|}$. Several works of Olson *et al.* [41,42] and Cohen [43,44] exploit the microcanonical ensemble to successfully yield accurate cross sections for the multiple-charged ion, ground-state atomic hydrogen systems in the ion-atom scattering problem. Recently, the classical trajectory ensemble approaches are also applied to the single/double ionization of a ground-state atom in an intense laser field, in which the classical results are comparable to quantum calculations and consistent with experiments [37,45].

In our case, in the center of mass coordinate system, we assume that the particle moves in the y-z

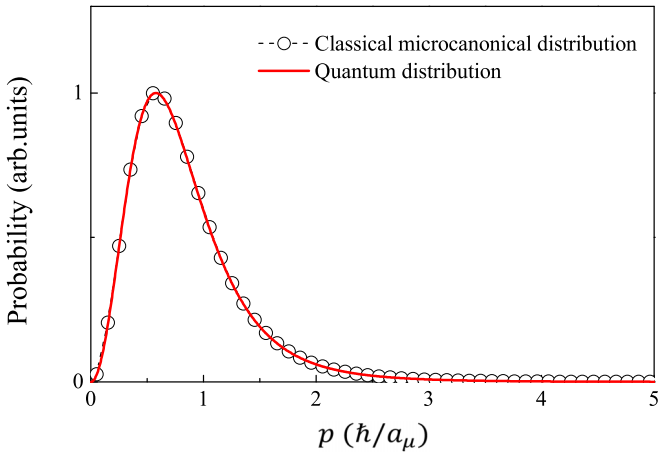

FIG. 2. The initial momentum distribution of the bounded muon given by the classical microcanonical distribution (the black circles) and the quantum distribution given by Eq. (3) (the red line), respectively.

plane and solve Kepler's equation to obtain the corresponding coordinates $\boldsymbol{r}_{y-z}^{\text{initial}} = [0, a\sqrt{1-\chi^2}\sin u, a(\cos u - \chi)]$ and momenta $\boldsymbol{p}_{y-z}^{\text{initial}} = [0, b\sqrt{1-\chi^2}\cos u/(1-\chi\cos u), -b\sin u/(1-\chi\cos u)]$ [43,46], where, $a = 1/(2E_{\text{g.s.}})$, $b = \sqrt{2E_{\text{g.s.}}}$, χ is the eccentricity of the orbit with χ^2 randomly distributed in [0, 1], and u is the eccentric angle. After performing an Euler rotation of the above orbit by $\boldsymbol{r}^{\text{initial}} = A\boldsymbol{r}_{y-z}^{\text{initial}}$, $\boldsymbol{p}^{\text{initial}} = A\boldsymbol{p}_{y-z}^{\text{initial}}$ (A is the Euler rotation matrix), the initialization of Tμ is completed. The center of mass of Tμ coincides with the coordinate origin [see Fig. 1(a)], thus the initial positions and momenta of triton and muon are $\boldsymbol{r}_{\mu}^{\text{initial}} = \frac{m_{\text{T}}}{m_{\text{T}}+m_{\mu}}\boldsymbol{r}^{\text{initial}}$, $\boldsymbol{r}_{\text{T}}^{\text{initial}} = -\frac{m_{\mu}}{m_{\text{T}}+m_{\mu}}\boldsymbol{r}^{\text{initial}}$, $\boldsymbol{p}_{\mu}^{\text{initial}} = \boldsymbol{p}^{\text{initial}}$, $\boldsymbol{p}_{\text{T}}^{\text{initial}} = -\boldsymbol{p}^{\text{initial}}$, respectively. The incident deuteron propagates along the z axis from $z_{\text{D}}^{\text{initial}} = 10^6$ fm or further; thus, the initial Coulomb energy can be safely ignored. The initial velocity of the deuteron is determined according to the kinetic energy as $v_{\text{D}}^{\text{initial}} = \sqrt{2E_{k0}/m_{\text{D}}}$. With the given initial conditions of the particles, the particle trajectories can be traced by numerically solving the canonical equations with the standard fourth–fifth order Runge-Kutta algorithm.

A typical trajectory of the D-Tμ collision is shown in Fig. 1(b), where the deuteron is closely approaching to Tμ and then bounced at the nearest distance between the DT nuclei of $r_{\text{DT}}^{\min}$. Quantum mechanics allows the nuclei to tunnel through the Coulomb barrier, permitting fusion reactions with energies smaller than the height of the barrier. We treat the minimum distance between the DT nuclei $r_{\text{DT}}^{\min}$ as the classical turning point and assume that the tunneling process is instantaneous; then, the penetrability is calculated according to the WKB formula [16,38]:

$$P_j = \exp\left\{-\frac{2}{\hbar}\int_{r_{\text{n}}}^{r_{\text{DT},j}^{\min}}\sqrt{2m\left[V(r) - V\left(r_{\text{DT},j}^{\min}\right)\right]}dr\right\}, \tag{4}$$

where $m = m_{\text{D}}m_{\text{T}}/(m_{\text{D}}+m_{\text{T}})$ is the reduced mass of the DT nuclei and $r_{\text{n}} = 3.89$ fm is their contact radius.

For a deuteron with a given initial kinetic energy, the classical turning point $r_{\text{DT},j}^{\min}$ of the D-Tμ scattering system has an Gaussian-like distribution [see Fig. 1(c)] and the statistical average penetrability can be obtained as follows:

$$P(\epsilon) = \frac{1}{N}\sum_{j=1}^{N} P_j(\epsilon), \tag{5}$$

where $\epsilon = E_{k0}(m_{\mu}+m_{\text{T}})/(m_{\mu}+m_{\text{T}}+m_{\text{D}})$ is the impact kinetic energy between the DT nuclei and N is the number of the classical trajectories. By employing the Gamow form [17,21,47], we obtain the DT fusion cross section as follows:

$$\sigma(\epsilon) = \frac{S(\epsilon)}{\epsilon}P(\epsilon), \tag{6}$$

where $S(\epsilon)$ is the astrophysical factor

$$S(\epsilon) = a + \frac{b}{\pi}\frac{d}{4(\epsilon-f)^2+d^2}. \tag{7}$$

The parameters $a = 118.8$ keV barn, $b = 8.647\times10^5$ keV^2 barn, $d = 45.05$ keV, and $f = 86.76$ keV, are obtained by fitting the experimental DT fusion cross-section data [17].

We apply our approach to study the dynamical process of the IFMCF in a laser field. The electric field of the laser is aligned parallel to the propagation direction of the incident deuteron [see Fig. 1(a)]. Simulations are performed with our proposed SC model, adding a laser field interaction term in the dipole approximation and length gauge [37]

$$V_{\text{interaction}} = -(q_{\text{D}}\boldsymbol{r}_{\text{D}} + q_{\text{T}}\boldsymbol{r}_{\text{T}} + q_{\mu}\boldsymbol{r}_{\mu})\boldsymbol{E}_{\text{laser}}, \tag{8}$$

where $\boldsymbol{E}_{\text{laser}}(t) = E_0 f(t)\sin(\omega t+\phi_0)\hat{e}_z$ is the laser electric field, ϕ_0 is the initial phase. The magnitude of the amplitude $E_0 = \sqrt{2I/\epsilon_0 c}$, where I is the laser intensity and c is the speed of light in vacuum. $f(t)$ denotes the field envelope and is formulated as follows:

$$f(t) = \begin{cases}\sin^2\frac{\omega t}{12} & \text{if } 0 \leqslant t \leqslant \frac{6\pi}{\omega},\\ 1 & \text{if } t > \frac{6\pi}{\omega}.\end{cases} \tag{9}$$

The field envelope is adiabatically activated with a three-cycle ramp and has a constant amplitude after the first three cycles. In our simulation, the time origin is set to be the moment when the laser is turned on [i.e., the laser pulse $f(t) = 0$], and the initial phase ϕ_0 is set randomly for each trajectory event.

III. MAIN RESULTS

In this section, within the framework of the developed SC model, we first discuss the screening effect of the muon on the DT fusion process. Then, we investigate how the laser field affects the fusion cross-section during IFMCF. Finally, we propose potential possible applications for enhancing the MCF cycles during the muonic lifetime.

A. IFMCF in the absence of a laser field

As depicted in Fig. 1(c), the classical turning points $r_{\text{DT},j}^{\min}$ of the D-Tμ collision system are closer than the minimum distance in bare DT collision system with the same impact kinetic energy ϵ (black dashed line), indicating that the negatively

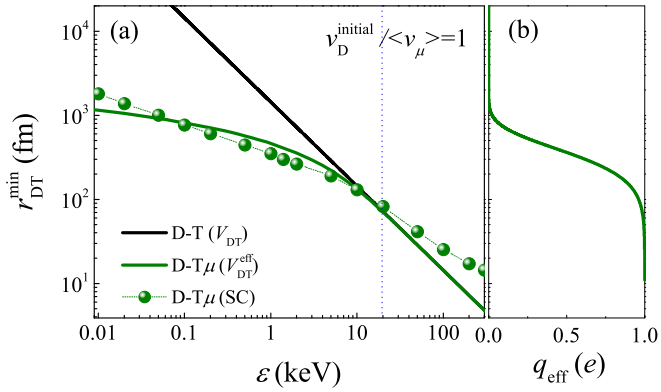

FIG. 3. (a) Dependence of the classical turning point on the impact kinetic energy ϵ, obtained by the SC method with the ensemble averaging (olive dot). The analytical results of a D-Tμ collision with an effective interaction potential V_{DT}^{eff} (olive line) and a bare DT collision with the Coulomb potential V_{DT} (black line) are also plotted for comparison. The blue dashed line indicates the incident energy $\epsilon = 19.5$ keV when the initial velocity of the deuteron is equal to the averaged rotation velocity of the muon. (b) The effective charge experienced by the incident deuteron in the D-Tμ scattering system as a function of r_{DT}.

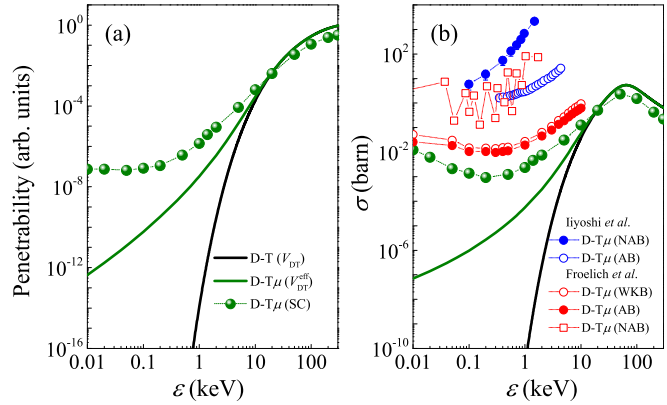

FIG. 4. (a),(b) Penetrability and DT fusion cross sections calculated from the SC model (olive solid circles) with respect to various impact kinetic energies ϵ. More than 10^5 classical trajectories are traced for each ϵ to obtain the results. To check the numerical convergence, we have doubled the number of trajectories and find that numerical fluctuations are distributed within the range of 3%–5%. The analytical results of V_{DT} and V_{DT}^{eff} are shown as the black and olive lines, respectively. The results obtained by Froelich *et al.* [49] using WKB (red open circles), adiabatic (AB, red solid circles), and nonadiabatic (NAB, red solid circles) methods, the results of Iiyoshi *et al.* [34] using AB (blue open circles) and NAB (blue solid circles) descriptions are presented for comparison, respectively.

charged muon screens the Coulomb repulsive potential between the DT nuclei, allowing the particles to approach each other more easily. We can estimate the charge distribution of a muon in a Tμ atom as

$$q_\mu^{eff} = q_\mu \int_0^{2\pi}\int_0^{\pi}\int_0^{r_{DT}} |\psi(r_{T\mu},\theta,\varphi)|^2 r_{T\mu}^2 \sin\theta dr_{T\mu} d\theta d\varphi = q_\mu\left[1-\left(1+\frac{2r_{DT}}{a_\mu}+\frac{2r_{DT}^2}{a_\mu^2}\right)\exp\left(-\frac{2r_{DT}}{a_\mu}\right)\right], \tag{10}$$

where $\psi(r_{T\mu},\theta,\varphi) = (1/\sqrt{\pi a_\mu^3})\exp(-r_{T\mu}/a_\mu)$ and $r_{T\mu} = |\mathbf{r}_\mu - \mathbf{r}_T|$, $r_{DT} = |\mathbf{r}_D - \mathbf{r}_T|$. Consequently, the actual amount of positive charge experienced by the incident deuteron in the D-Tμ scattering system can be calculated as

$$q_{eff} = q_T + q_\mu^{eff} = -q_\mu\left(1+\frac{2r_{DT}}{a_\mu}+\frac{2r_{DT}^2}{a_\mu^2}\right)\exp\left(-\frac{2r_{DT}}{a_\mu}\right). \tag{11}$$

Hence, the interaction potential between the DT nuclei can be treated as $V_{DT}^{eff} = q_D q_{eff} e^2/4\pi\varepsilon_0 r_{DT}$, which tends to the purely Coulomb potential $V_{DT} = q_D q_T e^2/4\pi\varepsilon_0 r_{DT}$ as $r_{DT} \to 0$.

The incident particle reaches the classical turning point when its initial kinetic energy is completely converted to the Coulomb potential [16]. Figure 3(a) demonstrates the classical turning point dependence of the initial kinetic energy ϵ for different interaction potentials V_{DT} and V_{DT}^{eff}. We also show the average $\bar{r}_{DT}^{min}$ of our SC simulation results as olive dots for comparison. For smaller incident energies, i.e., $\epsilon < 19.5$ keV, the SC simulation results agree with the analytical formula $\epsilon = V_{DT}^{eff}(r_{DT}^{min})$. Due to the high speed of the muon orbiting the triton, the deuteron cannot completely recognize the muonic motions as it travels and thus likely experiences a 'muon cloud' with a charge distribution of q_μ^{eff}. However, when the projectile velocity of the deuteron is larger than the averaged rotation velocity of the muon, i.e., $v_D^{initial}/\bar{v}_\mu > 1$ and $\epsilon > 19.5$ keV, the Coulomb attraction potential between μ and deuteron has a significant effect on the trajectory as the deuteron passes through the Tμ atom. As a result, the average classical turning point $\bar{r}_{DT}^{min}$ deviates from the analytical formula $\epsilon = V_{DT}^{eff}(r_{DT}^{min})$.

According to Eqs. (4) and (5), we can calculate the ensemble average penetrability versus the incident kinetic energy ϵ for different interaction potentials V_{DT} and V_{DT}^{eff} [the black and olive lines in Fig. 4(a), respectively]. We find that the penetrability in the D-Tμ collision system is considerably larger than that in a bare DT collision with the same ϵ due to the decrease in r_{DT}^{min}. Taking $\epsilon = 1$ keV as an example, the penetrability increases by nine orders of magnitude. In addition, the penetrability of the SC results tends toward an approximately fixed value as the incident energy ϵ decreases, which differs from the analytical prediction of the interaction potential $V_{DT}^{eff}(r_{DT}^{min})$. To understand the possible physical mechanisms underlying this result, we plot the corresponding distribution of r_{DT}^{min} for different incident energies in Fig. 5(a). We find that the r_{DT}^{min} distributions tend toward the same peak (shaded region) with decreasing ϵ, suggesting that the particle's trajectory converges to a minimum position of the order of 500 fm. This nearest position approximately corresponds to the equilibrium internuclear separation of a DTμ^+ molecular ion, which can be read out from the dissociation energy curve of $V_{DT\mu^+}$ by using the variational method [48]. Compared with the classical analytical predictions of V_{DT} and V_{DT}^{eff} as shown in Fig. 5(b), the $V_{DT\mu+}$ curve has a minimum value at $r_{DT} \approx 673$ fm, i.e., the DTμ^+ molecular ion might be formed during the collision process in the range $\epsilon < 0.1$ keV.

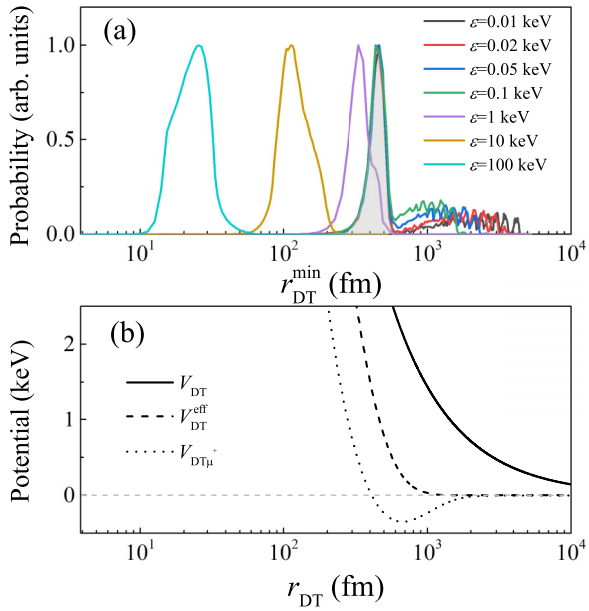

FIG. 5. (a) The distribution of the classical turning points for various incident energies. (b) Different potentials as a function of the relative distance r_{DT} between the DT nuclei.

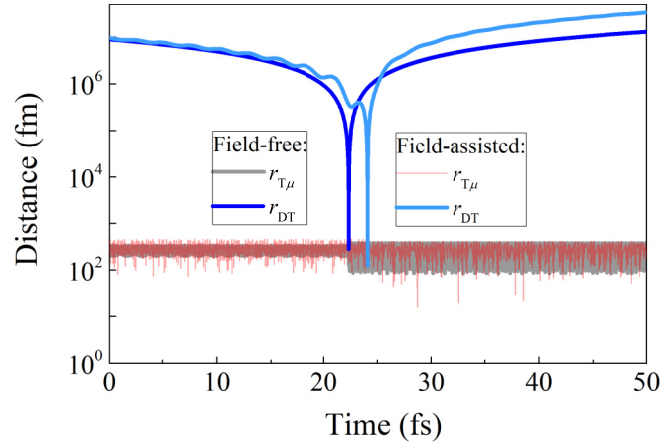

FIG. 6. Typical trajectory of a laser-assisted D-Tμ scattering system in comparison with the field-free case. The laser parameters are $\omega = 1.55$ eV and $I = 10^{20}$ W/cm^2, and the impact kinetic energy is $\epsilon = 1$ keV.

Some recent works have investigated the possibility of DT fusion by calculating the muonic atom-nucleus collision cross section, with the results suggesting that the fusion cross section increases substantially by up to 2000 barns within the range up to $\epsilon = 1.4$ keV [34]. We examine the DT fusion cross section σ in this IFMCF system with our SC approach. The DT fusion cross section σ according to the penetrability of a D-Tμ scattering system with the Gamow form described in Eq. (6) is shown in Fig. 4(b). The parameters in Eq. (7) are set to $a = 118.8$ keV barn, $b = 8.647 \times 10^5$ keV^2 barn, $d = 45.05$ keV, and $f = 86.76$ keV. These values were obtained by fitting the experimental data [13,17]. Our results qualitatively agree with early predictions by the WKB method [49] but deviate from the estimations described in Ref. [34] when the incident energy ϵ is less than 10 keV. Remarkably, since $P(\epsilon)$ tends toward a constant value in the range $\epsilon \lesssim 0.1$ keV, the cross section $\sigma(\epsilon)$ increases counterintuitively with decreasing incident energies ϵ. It probably indicates that treating the fusion problem in the D-Tμ system with the Gamow form is inapplicable in this tiny range.

B. IFMCF in the presence of intense laser field

Laser-assisted collisions have received a considerable amount of attention in recent decades. In this systems, the presence of an intense electromagnetic field modulates the cross sections of atomic ionizations or excitations [50–52] and the nuclear processes [16,53–55]. Here, we study a laser assisted D-Tμ collision system with our SC approach, focusing on effect of the laser field on the fusion cross sections of DT nuclei.

Taking $\epsilon = 1$ keV as an example, we illustrate the typical trajectories of a laser-assisted D-Tμ collision in Fig. 6. In the absence of laser field, the deuteron reaches the classical turning point of DT nuclei with $r_{\mathrm{DT}}^{\mathrm{min}}$ when its impact kinetic energy is completely converted to the Coulomb potential; then, the deuteron bounces back. In the presence of a laser field, the deuteron subjoins a quiver motion which leads to a smaller value of $r_{\mathrm{DT}}^{\mathrm{min}}$ during the collision process. The DT fusion probability is enhanced due to the closer classical turning point, as shown by Eqs. (4) and (6). Since we consider muonic atom-nucleus collision in this work, we restrict our simulations to situations in which the laser field is not strong enough to ionize the Tμ atom ($I < 10^{23}$ W/cm^2) [56]. Therefore, the influence of the laser field can be considered a perturbation of the motions of the muon and triton (red line in Fig. 6) that increases the effective incident kinetic energy of the deuteron during the collision.

In addition, the laser-field assisted $r_{\mathrm{DT}}^{\mathrm{min}}$ depends on the laser intensity I, frequency ω, and carrier phase ϕ_0. Figure 7(a) shows the phase-averaged fusion cross-sections σ of our SC calculation results for various laser parameters. Compared with the field-free case, in this scenario, σ increases rapidly with increasing laser intensity for a fixed ω. For a certain initial energy ϵ, the laser-enhanced fusion cross section tends toward a peak value as the intensity increases; thus, the DT nuclei approach each other with the contact radius of r_{n} during the collision process. Increasing the frequency of the laser field weakens this effect, which is derived from decreasing the quiver distance $r_{\mathrm{D}}^{\mathrm{quiver}} = q_{\mathrm{D}}E_0/m_{\mathrm{D}}\omega^2$ of deuteron. There exist the critical values of the laser intensity for various ω, beyond which the enhance effect of the lasers becomes significant. We numerically explore a wide range of laser parameters to determine the critical values and then show the phase diagram of the enhancement region in the parameter plane of the laser frequency and intensity in Fig. 7(b) accordingly. The region of effective enhancement is mainly found in the low-frequency and high-intensity regime and is approximately bounded by the scaled quiver velocity of the deuteron $\eta = q_{\mathrm{D}}E_0/m_{\mathrm{D}}\omega c \approx 0.0002$, e.g., the averaged quiver kinetic energy of deuteron in laser field $U_{\mathrm{p}} = (q_{\mathrm{D}}E_0)^2/4m_{\mathrm{D}}\omega^2 \approx 0.0187$ keV. The typical parameters of various laser facilities are displayed in Fig. 7(b).

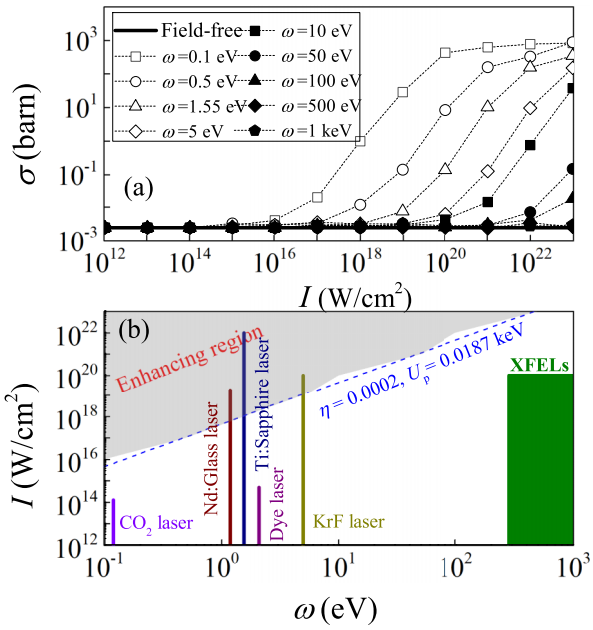

FIG. 7. (a) DT fusion cross sections with various laser intensities and frequencies. The impact kinetic energy is $\epsilon = 1$ keV. More than 10^5 classical trajectories are traced and associated average scheme is made to obtain each point. To check the numerical convergence, we have doubled the number of trajectories and find that numerical fluctuations are less than 5%. (b) Phase diagram of the effective region of the laser-field-enhanced DT fusion cross sections. The dashed blue line denotes $\eta = 0.0002$ and $U_p = 0.0187$ keV. Various laser facilities are shown for comparison and the specific parameters were obtained from Refs. [13,16].

Current intense laser facilities with frequencies in the near-infrared regime such as Nd:glass laser (with a peak intensity of 2×10^{19} W/cm^2 and a frequency of 1.18 eV) [57] and Ti:sapphire laser (with a peak intensity of 10^{22} W/cm^2 and frequency of 1.55 eV) [59] can effectively enhance the fusion cross section in IFMCF process.

Note that the classical three-body problem is a nonintegrable system and their involved trajectories might be unstable and chaotic. In fact, there also exists the chaotic behavior even in the two-body scattering in the presence of a laser field [58]. Nevertheless, one can obtain a definite physical result by averaging over these trajectories including chaotic ones as shown and carefully discussed in Ref. [58]. Here, we traced more than 10^5 classical trajectories of the D-Tμ scattering system for a certain projectile energy to guarantee the numerical convergence.

C. Application

We then estimate the number N of DT fusion reactions catalyzed by one muon during its lifetime in the laser assisted IFMCF system. For convenience, the fusion reactions were assumed occur in the gaseous deuterium-tritium mixture, and the density n_D of the deuterons coincides with the density $n_{T\mu}$ during the fusion process. Therefore, N can be approximately obtained as follows [36]:

$$N \approx n_D \sigma v \tau_\mu, \tag{12}$$

where $v = |\boldsymbol{v}_D - \boldsymbol{v}_{T\mu}| = \sqrt{2\epsilon/m_r}$ and $m_r = (m_T + m_\mu)m_D/(m_D + m_T + m_\mu)$. With a nonadiabatic calculation, Ref. [36] suggests that σ is about 2200 barn corresponding to $\epsilon \approx 1.5$ keV and obtained $N \approx 120$ for $n_D = 5 \times 10^{20}$ cm^{-3} according to Eq. (12). Some works have predicted that N can reach 1000 in a neutron source, such as an IFMCF reactor for the transmutation of long-lived fission products (LLFP) [34,35], in which the gas density can be increased to 10^{22} cm^{-3} by Mach shock wave using a supersonic stream. We also investigated the number of catalyzed fusion reactions N with our SC method. For instance, we consider $n_D = 5 \times 10^{21}$ cm^{-3} and $\epsilon = 1$ keV. According to Eq. (12), we obtain $N < 1$ in the field-free case, while $N \approx 380$ with the laser parameters of $I = 10^{22}$ W/cm^2 and $\omega = 1.55$ eV. Our results suggest that the laser assisted IFMCF process can achieve large number of fusion reactions catalyzed by the muon during its lifetime.

IV. CONCLUSIONS

In summary, we investigated the influence of intense laser fields on DT fusion cross sections in an IFMCF system. By tracing the classical trajectory of the D-Tμ collision process, we explain the shielding effect of muons catalyzing DT fusion processes when the impact velocity of the deuteron is considerably smaller than the average velocity of the muon in the bound state. Moreover, we predict that laser fields can enhance the fusion probability due to the closer tunneling distance between the DT nuclei. Our results provide insight into the underlying three-body dynamics and suggest fusion experimental testing based on the ultraintense laser facilities such as the extreme light infrastructure in future work [60,61]. In addition, muonic atoms and muonic molecules in intense laser fields are interesting subjects for future work, including high-order harmonic generation [62] and recollision physics [53], and we expect our SC model to have important applications in addressing such problems.

ACKNOWLEDGMENTS

This work is supported by funding from the National Natural Science Foundation of China (NSFC) (Grants No. 12174034, No. 12047510, No. 11822401, No. U1930402 and No. U1930403).

[1] M. Kikuchi, *Frontiers in Fusion Research* (Springer-Verlag, London, 2011).

[2] F. L. Hinton and R. D. Hazeltine, Rev. Mod. Phys. **48**, 239 (1976).

[3] J. Sheffield, Rev. Mod. Phys. **66**, 1015 (1994).
[4] J. Ongena, R. Koch, R. Wolf, and H. Zohm, Nat. Phys. **12**, 398 (2016).
[5] J. Nuckolls, L. Wood, A. Thiessen, and G. Zimmerman, Nature (London) **239**, 139 (1972).
[6] R. Betti and O. A. Hurricane, Nat. Phys. **12**, 435 (2016).
[7] D. Clery, Science **373**, 841 (2021).
[8] F. C. Frank, Nature (London) **160**, 525 (1947).
[9] J. D. Jackson, Phys. Rev. **106**, 330 (1957).
[10] W. P. S. Tan, Nature (London) **263**, 656 (1976).
[11] S. E. Jones, Nature (London) **321**, 127 (1986).
[12] F. Queisser and R. Schützhold, Phys. Rev. C **100**, 041601(R) (2019).
[13] W. J. Lv, H. Duan, and J. Liu, Phys. Rev. C **100**, 064610 (2019).
[14] X. Wang, Phys. Rev. C **102**, 011601(R) (2020).
[15] C. Kohlfürst, F. Queisser, and R. Schützhold, Phys. Rev. Res. **3**, 033153 (2021).
[16] S. W. Liu, H. Duan, D. F. Ye, and J. Liu, Phys. Rev. C **104**, 044614 (2021).
[17] S. Atzeni and J. Meyer-ter-Vehn, *The Physics of Inertial Fusion Beam Plasma Interaction, Hydrodynamics, Hot Dense Matter* (Clarendon, Oxford, 2004).
[18] B. H. Flowers, Proc. R. Soc. London, Ser. A **204**, 503 (1951).
[19] H. V. Argo, R. F. Taschek, H. M. Agnew, A. Hemmendinger, and W. T. Leland, Phys. Rev. **87**, 612 (1952).
[20] H. S. Bosch and G. M. Hale, Nucl. Fusion **32**, 611 (1992).
[21] E. M. Burbidge, G. R. Burbidge, W. A. Fowler, and F. Hqylk, Rev. Mod. Phys. **29**, 547 (1957).
[22] L. I. Ponomarev, Contemp. Phys. **31**, 219 (1990).
[23] V. V. Filchenkov, Phys. Part. Nucl. **47**, 591 (2016).
[24] C. DeW Van Siclen and S. E. Jones, J. Phys. G: Nucl. Part. Phys. **12**, 213 (1986).
[25] P. Baumann *et al.*, Phys. Rev. Lett. **70**, 3720 (1993).
[26] Y. Kino, M. R. Harston, I. Shimamura, E. A. G. Armour, and M. Kamimura, Phys. Rev. A **52**, 870 (1995).
[27] P. Froelich and J. Wallenius, Phys. Rev. Lett. **75**, 2108 (1995).
[28] M. C. Fujiwara *et al.*, Phys. Rev. Lett. **85**, 1642 (2000).
[29] S. E. Jones *et al.*, Phys. Rev. Lett. **56**, 588 (1986).
[30] S. Eliezer and Z. Henis, Fusion Technol. **26**, 46 (1994).
[31] R. Ackerbauer *et al.*, Nucl. Phys. A **652**, 311 (1999).
[32] K. Ishida, K. Nagamine, T. Matsuzaki, and N. Kawamura, J. Phys. G: Nucl. Part. Phys. **29**, 2043 (2003)
[33] N. Kawamura *et al.*, Phys. Rev. Lett. **90**, 043401 (2003).
[34] A. Iiyoshi, Y. Kino, M. Sato, Y. Tanahashi, N. Yamamoto, S. Nakatani, T. Yamashita, M. Tendler, and O. Motojima, AIP Conf. Proc. **2179**, 020010 (2019).
[35] N. Yamamoto, M. Sato, H. Takano, and A. Iiyoshi, Plasma Fusion Res. **16**, 1405074 (2021).
[36] M. L. Shmatov, Phys. Plasmas **28**, 124501 (2021).
[37] J. Liu, *Classical Trajectory Perspective of Atomic Ionization in Strong Laser Fields: Semiclassical Modeling* (Springer, New York, 2013).
[38] L. D. Landau and E. M. Lifshitz, *Quantum Mechanics Non-relativistic Theory* (Pergamon Press, London/Paris, 1958).
[39] R. Abrines and I. C. Percival, Proc. Phys. Soc. **88**, 861 (1966).
[40] R. Abrines, I. C. Percival, and N. A. Valentine, Proc. Phys. Soc. **89**, 515 (1966).
[41] R. E. Olson and A. Salop, Phys. Rev. A **16**, 531 (1977).
[42] R. E. Olson, J. Phys. B: At. Mol. Phys. **13**, 483 (1980).
[43] J. S. Cohen, Phys. Rev. A **26**, 3008 (1982).
[44] J. S. Cohen, Phys. Rev. A **27**, 167 (1983).
[45] W. Becker, X. J. Liu, P. J. Ho, and J. H. Eberly, Rev. Mod. Phys. **84**, 1011 (2012).
[46] J. G. Leopold and I. C. Percival, J. Phys. B: At. Mol. Phys. **12**, 709 (1979).
[47] G. Gamow, Z. Phys. **51**, 204 (1928).
[48] W. Greiner, *Quantum Mechanics-Special Chapters* (Springer-Verlag, Berlin, 1998).
[49] P. Froelich, A. Flores-Riveros, J. Wallenius, and K. Szalewicz, Phys. Lett. A **189**, 307 (1994).
[50] F. Ehlotzky, A. Jaroń, and J. Z. Kamiński, Phys. Rep. **297**, 63 (1998).
[51] S. W. Liu, D. F. Ye, and J. Liu, Phys. Rev. A **101**, 052704 (2020).
[52] C. Höhr, A. Dorn, B. Najjari, D. Fischer, C. D. Schröter, and J. Ullrich, Phys. Rev. Lett. **94**, 153201 (2005).
[53] S. Chelkowski, A. D. Bandrauk, and P. B. Corkum, Phys. Rev. Lett. **93**, 083602 (2004).
[54] H. M. C. Cortés, C. Müller, C. H. Keitel, and A. Pálffy, Phys. Lett. B **723**, 401 (2013).
[55] E. Lötstedt and K. Midorikawa, Phys. Rev. Lett. **112**, 093001 (2014).
[56] S. Augst, D. Strickland, D. D. Meyerhofer, S. L. Chin, and J. H. Eberly, Phys. Rev. Lett. **63**, 2212 (1989).
[57] J. Badziak, S. Jabłoński, P. Parys, A. Szydłowski, J. Fuchs, and A. Mancic, Laser Part. Beams **28**, 575 (2010).
[58] B. HuP, J. Liu, and S. G. Chen, Phys. Lett. A **236**, 533 (1997).
[59] S. W. Bahk, P. Rousseau, V. Chvykov, G. Kalintchenko, A. Maksimchuk, G. A. Mourou, and V. Yanovsky, Opt. Lett. **29**, 2837 (2004).
[60] C. A. Ur, D. Balabanski, G. Cata-Danil, S. Gales, I. Morjan, O. Tesileanu, D. Ursescu, I. Ursu, and N. V. Zamfir, Nucl. Instrum. Methods Phys. Res. B **355**, 198 (2015).
[61] Extreme Light Infrastructure (ELI), http://www.eli-np.ro.
[62] A. Shahbaz, C. Müller, A. Staudt, T. J. Bürvenich, and C. H. Keitel, Phys. Rev. Lett. **98**, 263901 (2007).